



# Seismic based characterization of total organic content from the marine Sembar shale, Lower Indus Basin, Pakistan

Omer Aziz<sup>1</sup> · Tahir Hussain<sup>1,2</sup> · Matee Ullah<sup>1,2</sup> · Asher Samuel Bhatti<sup>1,2</sup> · Aamir Ali<sup>1</sup>

Received: 9 December 2016 / Accepted: 8 February 2018 / Published online: 24 February 2018  
© Springer Science+Business Media B.V., part of Springer Nature 2018

## Abstract

The exploration and production of unconventional resources has increased significantly over the past few years around the globe to fulfill growing energy demands. Hydrocarbon potential of these unconventional petroleum systems depends on the presence of significant organic matter; their thermal maturity and the quality of present hydrocarbons i.e. gas or oil shale. In this work, we present a workflow for estimating Total Organic Content (TOC) from seismic reflection data. To achieve the objective of this study, we have chosen a classic potential candidate for exploration of unconventional reserves, the shale of the Sembar Formation, Lower Indus Basin, Pakistan. Our method includes the estimation of TOC from the well data using the Passey's  $\Delta\log R$  and Schwarzkopf's methods. From seismic data, maps of Relative Acoustic Impedance (RAI) are extracted at maximum and minimum TOC zones within the Sembar Formation. A geostatistical trend with good correlation coefficient ( $R^2$ ) for cross-plots between TOC and RAI at well locations is used for estimation of seismic based TOC at the reservoir scale. Our results suggest a good calibration of TOC values from seismic at well locations. The estimated TOC values range from 1 to 4% showing that the shale of the Sembar Formation lies in the range of good to excellent unconventional oil/gas play within the context of TOC. This methodology of source rock evaluation provides a spatial distribution of TOC at the reservoir scale as compared to the conventional distribution generated from samples collected over sparse wells. The approach presented in this work has wider applications for source rock evaluation in other similar petroliferous basins worldwide.

**Keywords** Shale gas · TOC · Passey's  $\Delta\log R$  method · Schwarzkopf's method · Relative acoustic impedance · Correlation coefficient

## Introduction

The ever-increasing demand of energy requires a deep insight into all possible ways of fulfilling it. One of the major components of the global energy mix comes from the exploitation of conventional resources (Bocora 2012; Zou et al. 2016). The increasing rate of the hydrocarbon production from conventional resources show continuous depleting trend for over 50 years (Miller and Sorrell 2014). Hence, there is a strong impetus to explore the hydrocarbon potential of unconventional resources i.e. oil/gas shales. Furthermore, the rise of unconventional resource exploitation

could present a new era in the overall global energy mix (Kefferpütz 2010; Sunjay 2011; Bocora 2012; Rezaee 2015).

Conventionally, shale is a source rock for petroleum systems, showing low permeability (Gluyas and Swarbrick 2009; Liu et al. 2012; Rezaee 2015). Contemporary geophysical and geological techniques have been focused on extracting hydrocarbons from clastics and carbonates due to their favorable permeability. With advances in hydrocarbon exploration techniques in the last few decades, it is now possible to extract hydrocarbons directly from source rocks (Kefferpütz 2010; Bocora 2012; Rezaee 2015).

The Total Organic Content (TOC) in shale, its thermal maturity and good porosity are key parameters for the generation and accumulation of hydrocarbons (Rybach 1986; Wood 1988; Wandrey et al. 2004; Gluyas and Swarbrick 2009; Rezaee 2015). Additionally, the vertical and lateral extent of source rocks can be identified and mapped by using seismic and well data (Løseth et al. 2011; Rezaee 2015). In fact, TOC content can be precisely determined at boreholes

✉ Aamir Ali  
aamirali.geo@gmail.com

<sup>1</sup> Department of Earth Sciences, Quaid-i-Azam University, Islamabad, Pakistan

<sup>2</sup> Department of Geology, Bacha Khan University, Charsadda, Pakistan

using different techniques such as Passey et al. (1990), Schwarzkopf (1992) and Bowman (2010) etc., and via the analysis of rock samples. This TOC distribution can be further mapped and extended with confidence away from control points on the reservoir scale using seismic data (Løseth et al. 2011; Rezaee 2015).

The objective of the paper is to evaluate the hydrocarbon potential of Sembar Formation in the Badin area of the Lower Indus Basin, Pakistan (Fig. 1), by mapping the TOC content using seismic and well log data within the context of unconventional resource production. Pakistan is endowed with 51 Trillion Cubic Feet (TCF) of recoverable gas shale reserves (Rezaee 2015). Shale of Sembar Formation is considered to be the most potential candidate in the region, with favorable characteristics, in terms of thickness, TOC values, and thermal maturity (Wandrey et al. 2004). The workflow followed in the present study is given in Fig. 2. The data used in this study comprises of 3-D seismic data (13 × 13 km<sup>2</sup>) and well log/vertical seismic profiling (VSP) data recorded in three wells (A, B and C) (Fig. 3).

### Geological setting

The study area is located about 160 km East of Karachi in the Lower Indus Basin, between Latitude 24°5'N–25°25'N and longitude 68°21'E–69°20'E (Fig. 1; Kadri 1995; Alam et al. 2002; Ahmad et al. 2011; Munir et al. 2014). The evolution of the Lower Indus Basin began in the Cretaceous, when the tectonic activity occurred in the Indus Basin forming a rift zone (Farah et al. 1984). This rift zone exists near the Thar Platform in the form of Sargodha High dividing the Indus Basin into the Upper and the Lower Indus Basins (Kadri 1995). As a consequence of this rifting and doming, mainly horst and graben structures are present below the Paleogene unconformity including Cretaceous and older strata (Alam et al. 2002). The effect of rifting and doming on our study area (eastern side of Lower Indus Basin) is relatively small, as it lies away from the main deformational zone. The extensional deformational rate increases from east to west and a large area of the eastern Lower Indus Sub-Basin (Badin) is dominated by tilted normal faults (Farah et al. 1984; Kadri 1995). These faults can be seen and mapped on seismic data

**Fig. 1** Map showing tectonics and regional geological setting of Pakistan including our study area (highlighted) situated in the Lower Indus Basin (Kazmi and Snee 1989)

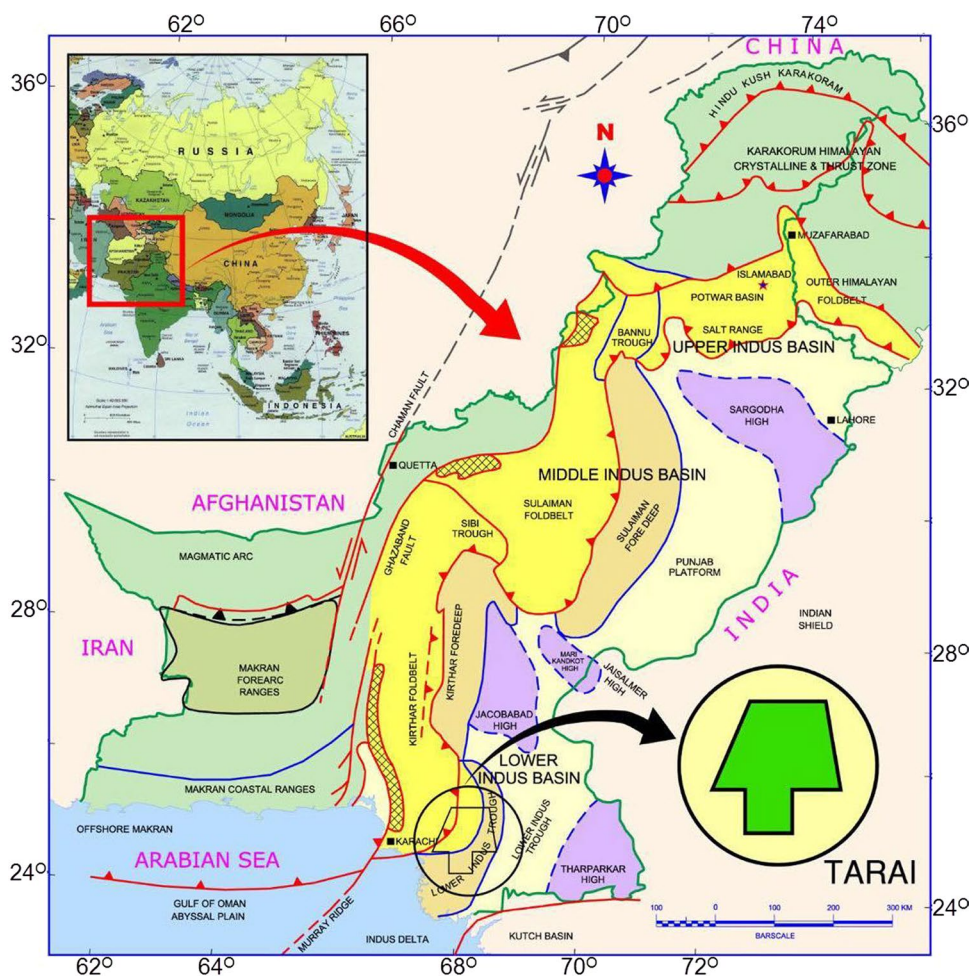
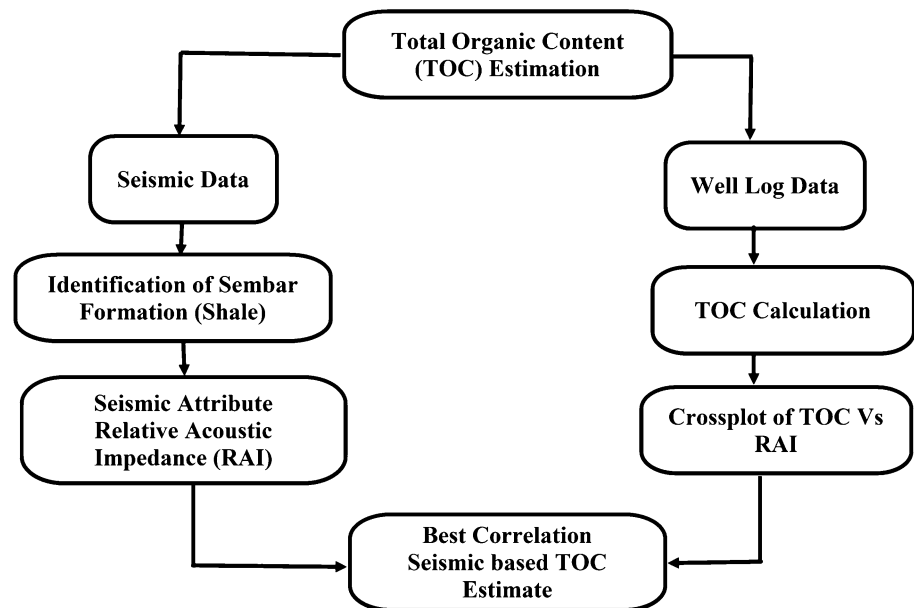


**Fig. 2** Flowchart of methodology followed in this study



which have deformed the Cretaceous and older strata (Kadri 1995).

Stratigraphically, the Indus Basin ranges from Cambrian to Holocene in age with erosional and non-depositional intervals, while in study area it ranges from Jurassic to Paleogene as shown in Fig. 4 (Alam et al. 2002). The depositional environment of the Cretaceous Sembar and Goru Formations is shallow marine in nature (Iqbal and Shah 1980). These formations are deposited over the regional erosive surface of Chiltan limestone (Jurassic age) along passive continental margins (Iqbal and Shah 1980). The Sembar Formation is a clastic rock with a large quantity of shale and a minor amount of siltstone and sandstone while Goru formation is a mixture of interbedded shale and sandstone (Fig. 4; Iqbal and Shah 1980; Raza et al. 1990). The shelf to shallow-marine depositional environment persisted till Late Cretaceous time, represented by the carbonates of the Parh, Moghal Kot and Fort Munro Formations. The Pab Formation hosts regressive sand, thus representing a change to a nearshore environment (Wandrey et al. 2004).

The Sembar, Goru and Ranikot Formations are major potential conventional/unconventional sources of the Lower Indus Basin (Ahmad et al. 2011; Abbasi et al. 2014). The hydrocarbon potential of the Sembar Formation in the northern Kirther range is low but improves towards the south and southeast (Eckhoff and Alam 1991). Lithologic composition of the Sembar Formation is variable in different areas (Ahmad et al. 2011). The average composition includes Quartz 42%, Clay 47%, Calcite 10% and Pyrite 1% (Ahmad et al. 2011). The gas content is also variable in the basin with  $1% < \text{CO}_2 < 70%$ ,  $1% < \text{N} < 80%$  and  $0.1% < \text{H}_2\text{S} < 13%$ . The Sembar Formation extends towards the southern parts of Pakistan and into the offshore area (Eickhoff and Alam 1991;

Shahzad et al. 2017). In the western side of the Lower Indus Basin, units of the same age (Kzhdumi, Garau and Gadvan Formations) continue into Iran in the Zagros fold-belt and the Persian Gulf Basin (Opera et al. 2013). These Formations possess potential source character in their respective basins within the context of unconventional resource exploitation (Opera et al. 2013). On the eastern side of the Lower Indus Basin, the Indian Rajasthan Basin comprises of lithological units, owing to the same depositional and tectonic history (Biswas 1987; Klett et al. 2011).

## Data and approach

In this research, we have devised a methodology for TOC estimation in the Sembar Formation in Badin area, Lower Indus Basin, Pakistan using 3-D seismic data together with well log data of the three wells (A, B and C). The 3-D seismic cube is acquired and processed using bin size of  $25 \times 25 \text{ m}^2$  and frequency range of 8–45 Hz, however this data can best resolve the target depth at frequency range of 10–35 Hz. The well data used, comprises of gamma ray (GR), spontaneous potential (SP), caliper (CALI), resistivity, density (RHOB), sonic (DT) and neutron porosity logs.

An indirect method is used for the estimation of TOC using well log data, which is an integral part for our proposed methodology. There exist many techniques for estimation of TOC from well log data such as Ferlt and Rieke (1980), Schmoker (1981), Meyer and Nederlof (1984), Fertl and Chilingier (1988), Passey et al. (1990), Myers and Jenkyns (1992), Schwarzkopf (1992) and Guidry and Walsh (1993). The contrast in geophysical response of a mature source rock, as compared to a non-source rock,

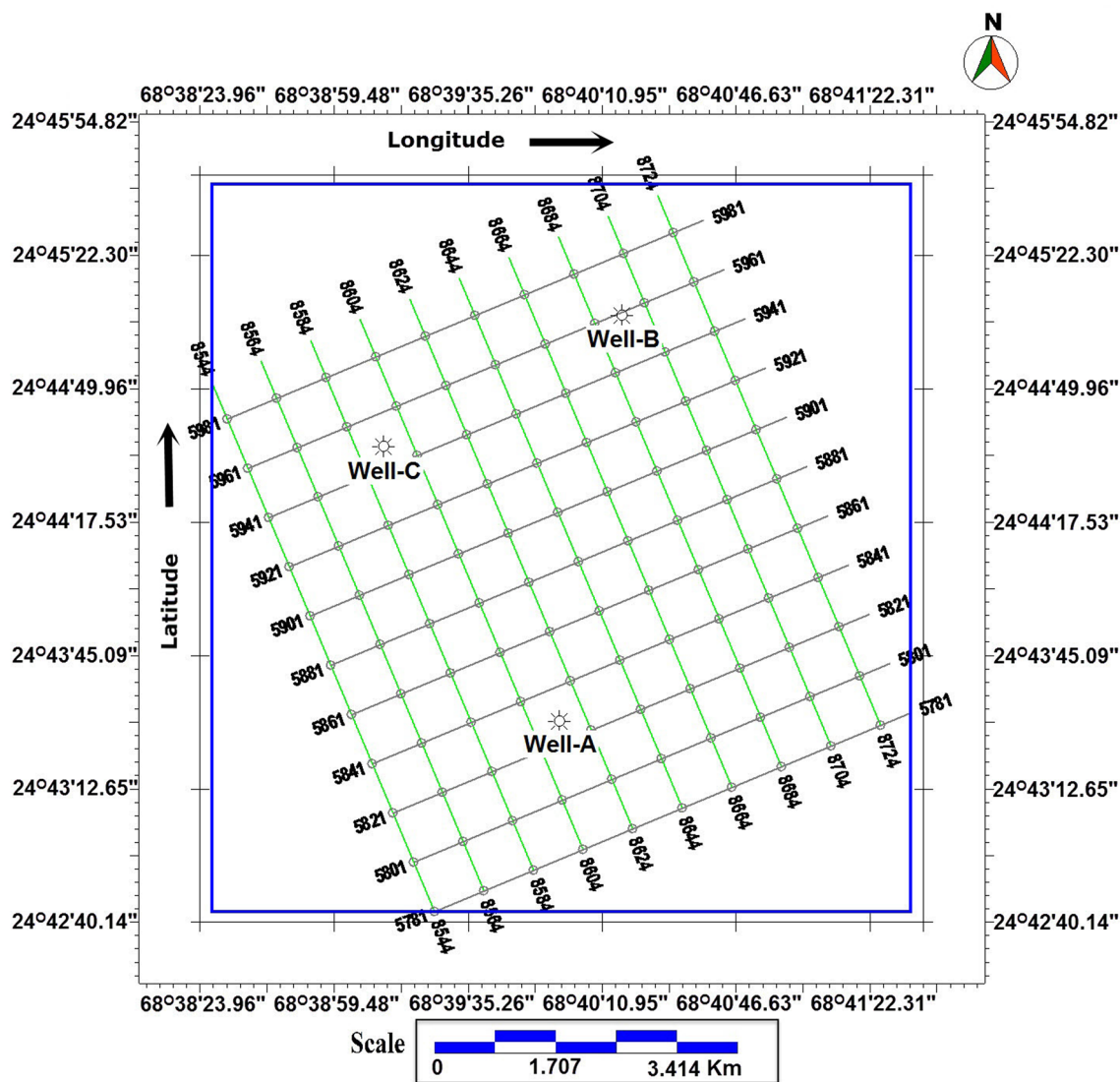


**Fig. 3** Base map of the Badin area with in-lines (gray) and cross-lines (green) including three wells (Well A, Well B and Well C)

provides the basis for these indirect techniques (Meyer and Nederlof 1984; Passey et al. 1990; Myers and Jenkyns 1992; Schwarzkopf 1992).

A substantial amount of organic matter in a mature source rock is converted to gaseous or liquid hydrocarbon, displacing formation water from the pores, and later revealing anomalous behavior on well logs (Philippi 1968; Nixon 1973; Meissner 1978). For example, resistivity, DT, neutron and GR logs show relative increase in the interval of mature source rocks, while density log response shows a decrease in mature source rock intervals, as described in Table 1 (Passey et al. 1990). In this study we have followed the approaches presented by Passey et al. (1990)

and Schwarzkopf (1992) for the estimation of TOC from well log data.

Reflection seismology (seismic methods) is one of the most important methods for the delineation of subsurface rock properties over larger extents despite its comparatively low resolution. On the other hand, well log/core data with relatively high resolution provides reliable information, but only for very small areal extents i.e. near the boreholes. The uncertainty in the rock property modeling increases as the distance from borehole increases. That is the point where seismic measurements in conjunction with rock physics modeling are very useful and its calibration with available well data can provide us a reliable model at the reservoir scale. The workflow followed in the current study is presented in Fig. 2 and detailed below.

**Fig. 4** Generalized stratigraphic chart of the study area (Alam et al. 2002; Abbasi et al. 2014, 2016)

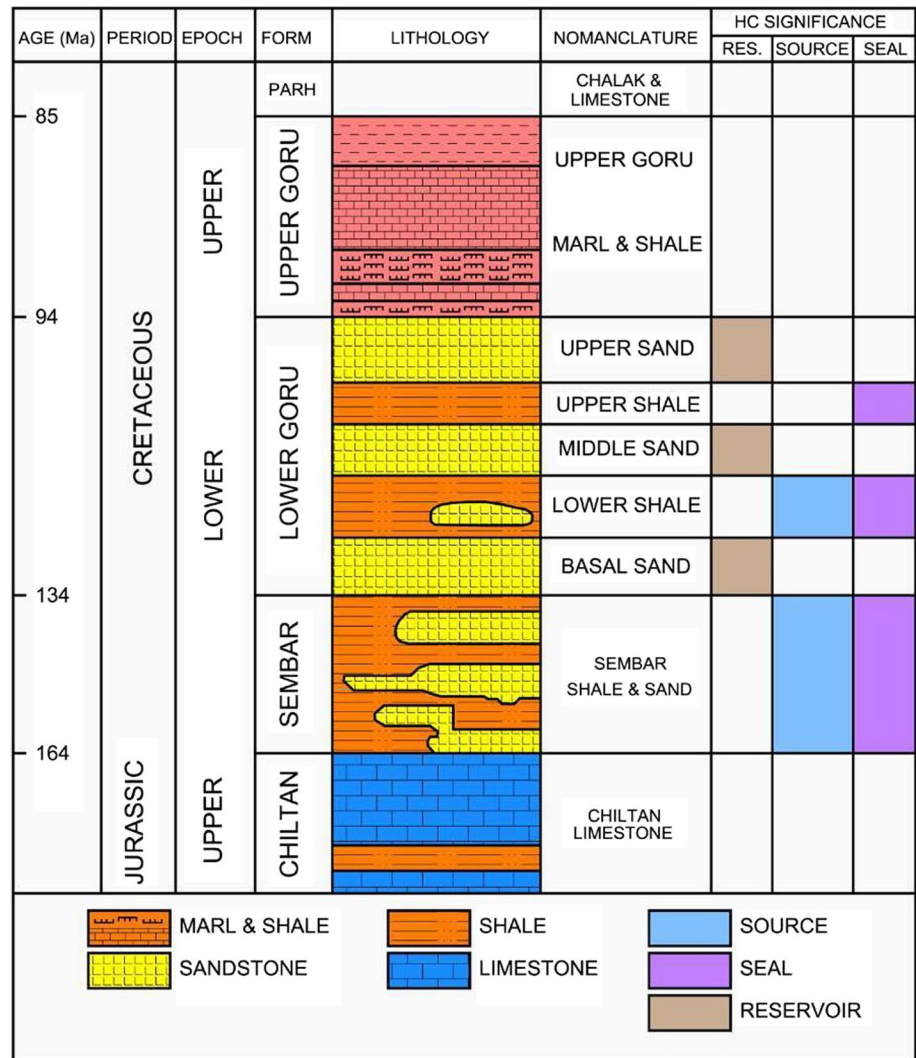


**Table 1** Responses of five conventional logs in the organic matter of source rock, in which only density response is low and other four logs (GR, DT, neutron and resistivity) have high response (Fertl and Chilingar 1988; Passey et al. 1990)

Logging tool	Response	Comments
Natural gamma ray	High	When uranium contents are highly concentrated in type-II kerogen
Total gamma ray	High	Presence of high amount of uranium makes the total gamma ray reading high. The high amount of uranium represents rich organic matter
Bulk density	Low	Because organic matter are less dense, so bulk density response decreases in organic rich rocks
Sonic transit time	High	Density of Kerogen is low, so the acoustic velocity in organic rich source rock decreases and as a result sonic transit time increases
Resistivity	High	Organic matters are bad conductors, so their resistivity is very high. Maturity and conversion of hydrocarbons within the source rock possess a direct relation to resistivity

**Demarcation of Sembar Formation**

Seismic reflection data is used to understand the regional distribution of the Sembar Formation in combination with well log data (Fig. 3). The top and base of the Sembar Formation are identified/marked on seismic data using

the available well tops and is confirmed through synthetic seismograms (well-to-seismic tie) generated from well log and VSP data. Time and depth contour maps are prepared from the top and bottom of the Sembar Formation to identify the lateral and vertical trend in the study area. Horizon based Relative Acoustic Impedance (RAI) attribute for the

Sembar Formation is applied to trace any acoustic impedance variations and to map TOC at reservoir scale.

### Passey overlay technique

In the  $\Delta\text{LogR}$  method, resistivity logs are superimposed to one of three porosity logs (neutron, DT and RHOB) (Passey et al. 1990; Liu et al. 2012). Resistivity logs are plotted on logarithmic scale and other logs (neutron, RHOB and DT logs) are displayed on linear scales (Rider 2002). Any combination of two logs can be taken i.e. resistivity/DT, resistivity/neutron or resistivity/RHOB. In this method, the neutron and RHOB logs are mostly affected by borehole wall rugosity, and it is better to use a combination of resistivity/DT for more precise results (Liu et al. 2012). Resistivity and DT curves are relatively scaled so that 100  $\mu\text{s}/\text{ft}$  of sonic data is equal to two logarithmic cycles of resistivity data (i.e. 100  $\mu\text{s}/\text{ft} = 2 \Omega\text{m}$  or 50  $\mu\text{s}/\text{ft} = 1 \Omega\text{m}$ ). Jianliang et al. (2012) also used GR logs by keeping similar scale factors for sonic data (50 API = 1  $\Omega\text{m}$ ).

The interval in which both curves are superimposed is known as a baseline. The baseline is mostly established in a fined grained non-source rock where both curves are on

the top of each other with small or zero separation. The separation between the curves in the source rock is called  $\Delta\text{LogR}$  which can be calculated mathematically as:

$$\Delta\text{LogR}_{\text{DT}} = \text{Log}_{10}\left(\frac{R}{R_{\text{Baseline}}}\right) - 0.02 \times (\Delta t + \Delta t_{\text{Baseline}}). \quad (1)$$

here  $\Delta\text{LogR}_{\text{DT}}$  reflects the separation between DT and resistivity logs,  $R$  is the true resistivity from LLD or ILD resistivity logs,  $R_{\text{Baseline}}$  is the value of resistivity corresponding to sonic transit time at baseline,  $\Delta t$  is the sonic transit time and  $\Delta t_{\text{Baseline}}$  is the value of sonic transit time corresponding to resistivity at the baseline. The constant value 0.02 is the scaling factor. Using  $\Delta\text{LogR}_{\text{DT}}$ , TOC can be estimated as:

$$\text{TOC}_{\text{DT}} = \Delta\text{LogR}_{\text{DT}} \times 10^{(2.297 - 0.1688 \times \text{LOM})}. \quad (2)$$

The  $\text{TOC}_{\text{DT}}$  is the TOC calculated using DT log, and LOM is the level of organic maturity. LOM values can be best obtained from core data. Whenever core data are not available, then conodont alteration indexes and Hood et al. (1975) charts can be used for LOM calculation, provided that vitrinite reflectance data is available (Passey et al. 1990).

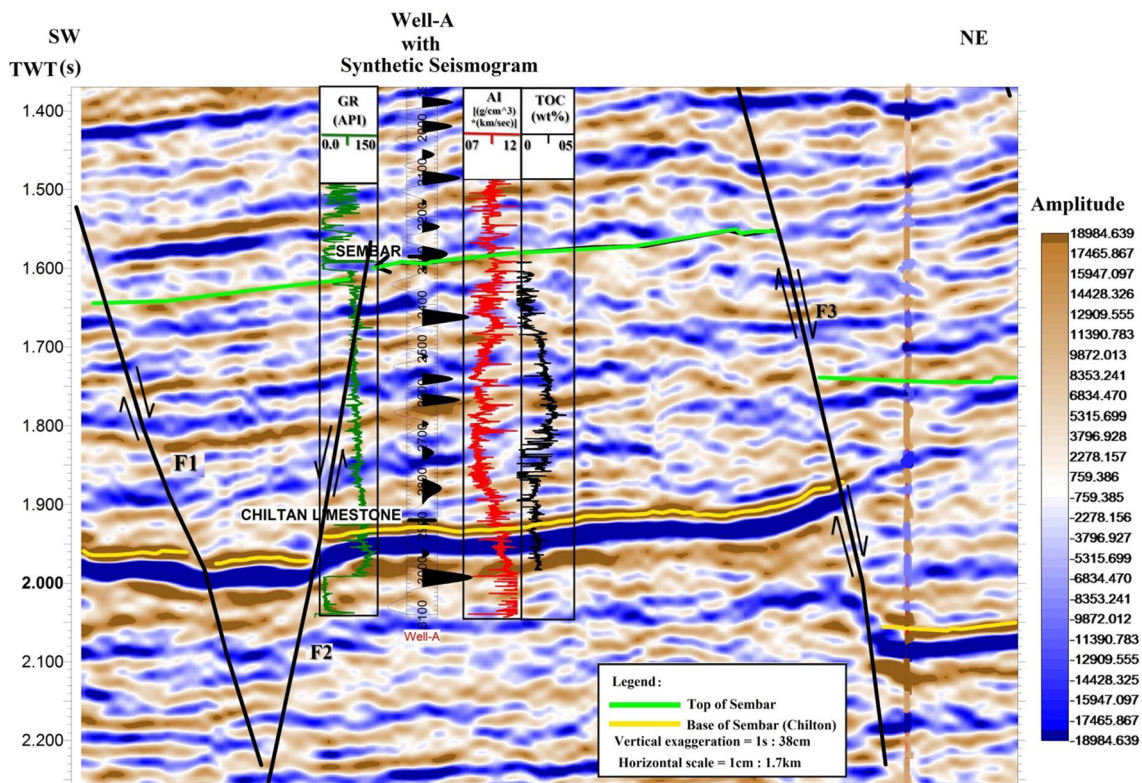


**Fig. 5** Superimposing synthetic seismogram over the seismic section of in-line 5821 along with GR log of well A. GR log is used here for differentiating/demarcating shaley intervals over seismic section. The

AI from well A is also displayed for calibration purpose. *F1*, *F2* and *F3* represent the faults having normal sense of shear

It is important to remember that TOC content and the maturity of the source rocks are directly proportional to the  $\Delta\log R$  separation. A large separation indicates large amounts of organic matter and high maturity for source rocks (Passey et al. 1990).

### Schwarzkopf's technique

For application of Schwarzkopf's technique, we have followed the approach presented by Myers and Jenkyns (1992). This approach requires a few assumptions before the application of its mathematical relations. The assumptions are: (1) the source rock comprises mud rock as the matrix with density of  $2.70 \text{ g/cm}^3$ , water filled density of  $1.05 \text{ g/cm}^3$  and kerogen density of  $1.1$  or  $1.2 \text{ g/cm}^3$ , (2) porosity and density of the source and non-source interval are same. The porosity for water filled pores ( $\phi_{fl}$ ) and kerogen ( $\phi_{ker}$ ) are estimated using the relations given below:

$$\phi_{fl} = \frac{\rho_{ns} - \rho_{ma}}{\rho_{fl} - \rho_{ma}} \tag{3}$$

and

$$\phi_{ker} = \frac{\rho_s - \rho_{ma}}{\rho_{ker} - \rho_{ma}} \tag{4}$$

The  $\rho_{ns}$  is the density of non-source interval (average from log) in  $\text{g/cm}^3$ ,  $\rho_s$  is the density of source interval (from log) in  $\text{g/cm}^3$ ,  $\rho_{ma}$  is the assumed mud rock density,  $\rho_{fl}$  is the assumed water filled density and  $\rho_{ker}$  is the assumed kerogen density. Finally, TOC in wt% can be estimated using the following relation:

$$\text{TOC} = \frac{0.85 \times \rho_{ker} - \phi_{ker}}{\rho_{ker} (\phi_{ker}) + \rho_{ma} (1 - \phi_{fl} - \phi_{ker})} \tag{5}$$

### Seismic based TOC estimation

Since acoustic impedance depicts elastic behavior of a material, it therefore should provide information about variations in lithology, mineralogy, and fluid constituents etc. across

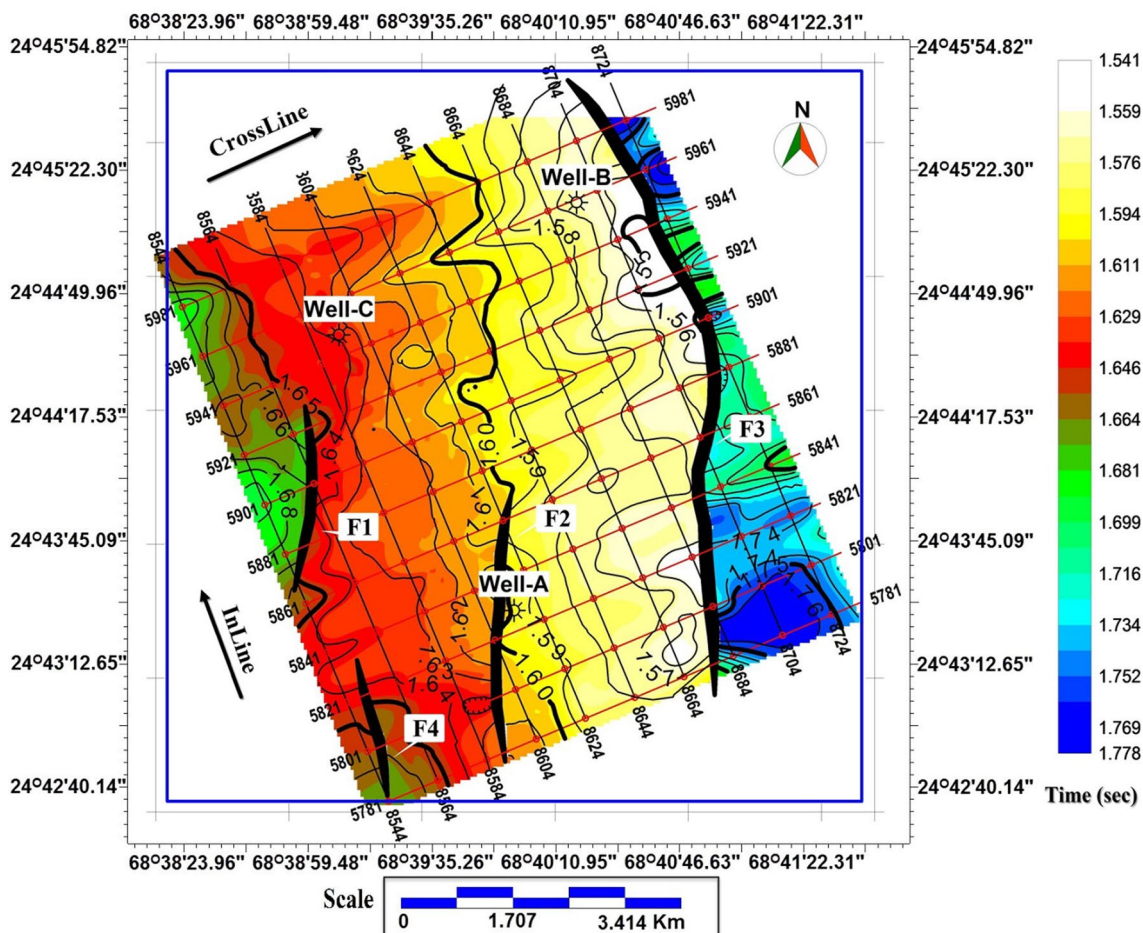


**Fig. 6** Time contour map from the top of Sembar Formation with contour interval of 0.01 s. *F1, F2, F3 and F4* represents faults traced over the base map. The color legend provides the information about shallowest and deepest parts of the Sembar Formation

the rock unit (Løseth et al. 2011). Moreover, the organic rich source rocks have low densities and acoustic impedances due to the high percentage of TOC compared to the non-source rock with a similar composition (Løseth et al. 2011). To evaluate the source rock potential of the Sembar Formation in Badin area, the zero phase band limited 3-D seismic data of the area is converted from amplitude to RAI using the relation given by Nissen et al. (2009)

$$\ln(\rho V) = 2 \int_{t=0}^{t=T} f(t) dt, \tag{6}$$

where  $f(t)$  is the band limited reflectivity series,  $\rho$  is density and  $V$  is the compressional wave velocity within the rock layer. The curves of estimated TOC and acoustic impedance (AI) from wells are calibrated with the RAI section. Subsequently, horizon/reflection having low RAI and high TOC is identified throughout the seismic cube within the Sembar Formation with the help of calibrated AI and TOC curves derived from the well log data. After that, RAI is

extracted along that interpreted horizons on a grid interval of  $25 \times 25$  m. The choice of this grid interval is based on the fact that the bin size used in the processing of the 3-D seismic volume is  $25 \times 25$  m and this grid interval is able to capture all the finer variations (in terms of RAI) within the data. Furthermore, RAI extracted in this way comes only from the rich TOC zone having low acoustic impedance within the Sembar Formation.

Similarly, for the sake of comparison, a particular horizon/reflection within the Sembar Formation having high acoustic impedance and low TOC is identified throughout the seismic cube with the help of AI and TOC from well log data, and RAI is extracted and gridded ( $25 \times 25$  m) along this horizon as discussed above.

In the next step, for the estimation of TOC from seismic data, a relationship describing the general trend between TOC (well derived property) and RAI (seismic derived property) is required. A relationship is established via a cross-plot between TOC and extracted RAI at the location of the wells for the high/low zones of TOC and RAI within

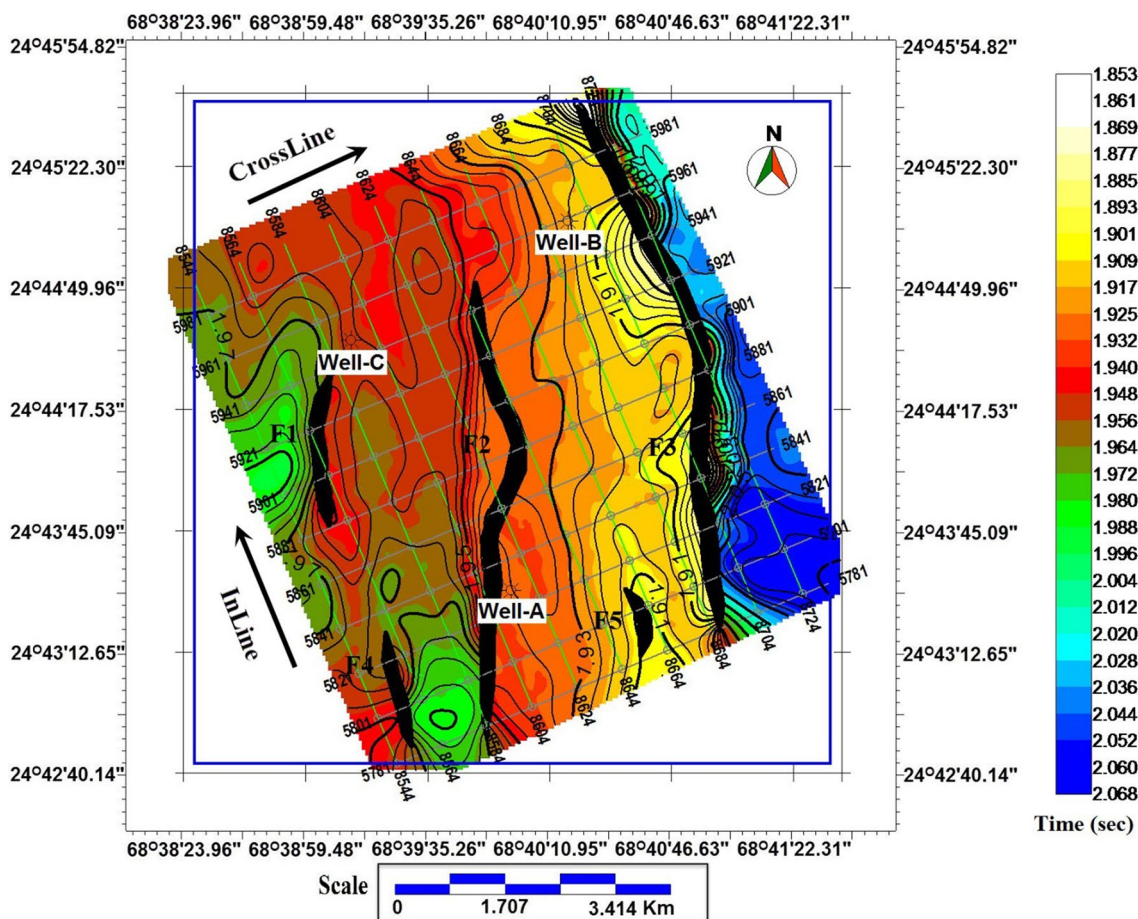


**Fig. 7** Time contour map from the bottom of the Sembar Formation with contour interval of 0.05 s. *F1, F2, F3, F4* and *F5* represents faults traced over the base map. The color legend provides the information about shallowest and deepest parts of the Sembar Formation



the Sembar Formation, which is then used for the conversion of RAI at reservoir scale to TOC.

### Results

In this research, we have devised a methodology for TOC estimation in the Sembar Formation in Badin area, Lower Indus Basin using 3-D seismic data together with well log data. The results are presented in the relevant sub headings below.

#### Spatial extent of the Sembar Formation

A synthetic seismogram is generated using DT and RHOB logs of Well A, and is correlated with the 3-D seismic data of Badin area with a correlation coefficient of  $R^2 = 0.93$  (Fig. 5). The top (1.6 s TWT) and bottom (1.94 s TWT) of the Sembar Formation is marked (Fig. 5) and the time structural maps from the top/bottom of the

Sembar Formation are prepared using contour intervals of 0.01 and 0.05 s respectively (Figs. 6, 7). As the generated contour maps from both top/bottom of the Sembar Formation reflect the same deformational style (Figs. 6, 7), therefore, only top and bottom of the Sembar Formation is mapped. However, it's not a usual case to map the top/bottom of the target zone only, if the structural complexity exists within the target zone (Bacon et al. 2007). For delineation of exploitation depth, the time structural map generated from the top of the Sembar Formation is converted using velocity derived from seismic and well data (Fig. 8). Furthermore, the time and depth contour maps show the spatial variation of Sembar Formation along with its deformational style. The thickness of Sembar Formation is interpreted to be  $\approx 366\text{--}546$  m based on the isopach grid map (Fig. 9), starting from the depth of around 2200 m with reference to the datum surface in the study area (Fig. 8). It is further inferred from the contour maps that the depth of Sembar Formation increases from east to west with normal faulting resulting in horst and

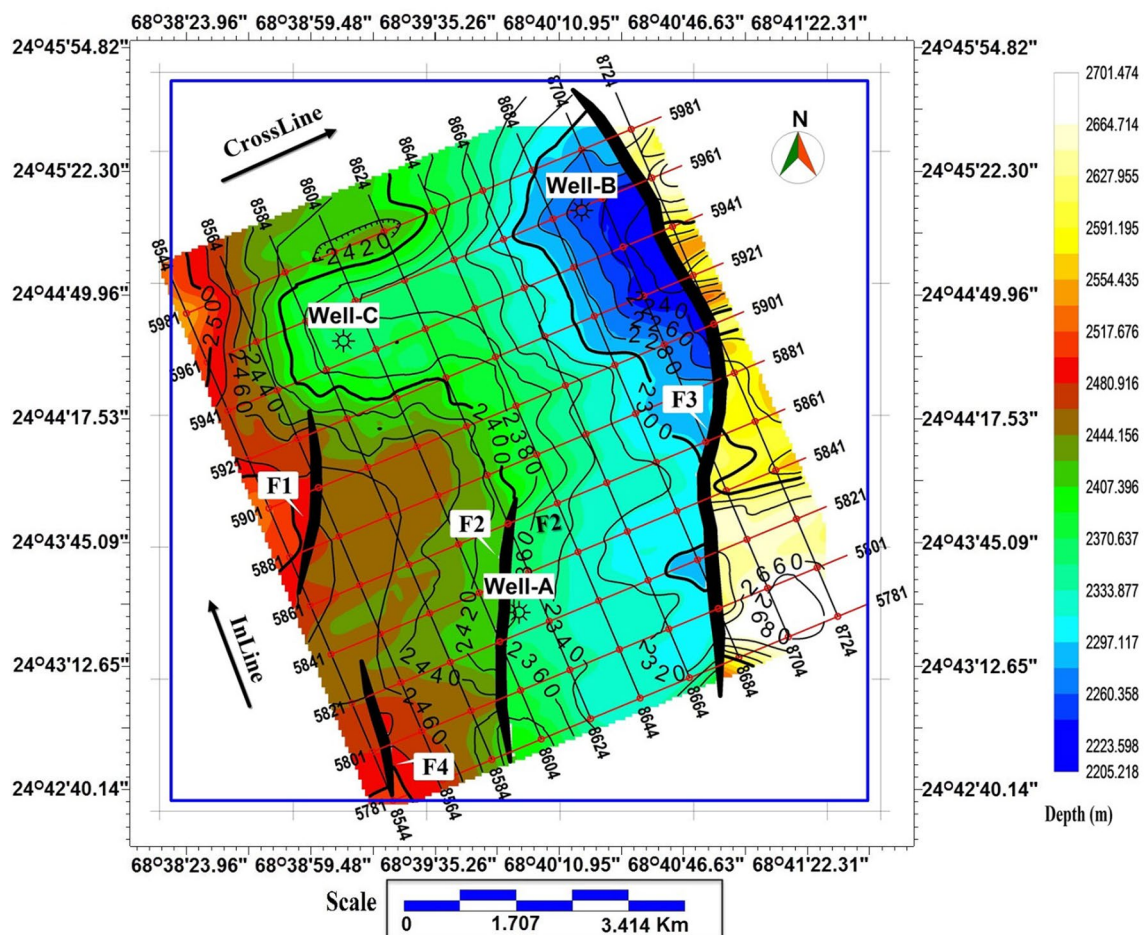


**Fig. 8** Depth contour map from the top of Sembar Formation with contour interval of 15 m. *F1, F2, F3* and *F4* represent the faults traced over the base map. The color legend provides the information about shallowest and deepest parts with of the Sembar Formation

graben structural patterns. Due to the depth and thickness of the Sembar Formation, it has high temperature and overburden pressure, which makes it an ideal source rock within the context of shale gas exploration.

**Logs based TOC estimation**

The well log data of three wells (A, B and C) are used for TOC (wt%) estimation of Sembar Formation by using Passey  $\Delta\log R$  and Schwarzkopf methods as discussed in Sections "Passey overlay technique and Schwarzkopf's Technique" (Table 2; Figs. 10, 11 and 12). In the source

rock interval, only the density log shows a decreasing trend, while the response of other logs such as GR, resistivity, DT and neutron shows an increasing trend, marking a rich TOC interval (Table 1; Passey et al. 1990, 2010). A baseline is established in all the three wells based on small or no separation between DT and resistivity logs. There is a 250–300 m interval at the center of the Sembar Formation having TOC values in the range of 1–4 wt% (Figs. 10, 11 and 12). Based on the estimated TOC within the Sembar Formation, the source rock interval can be designated as having TOC > 1 and the non-source interval as having TOC < 1.

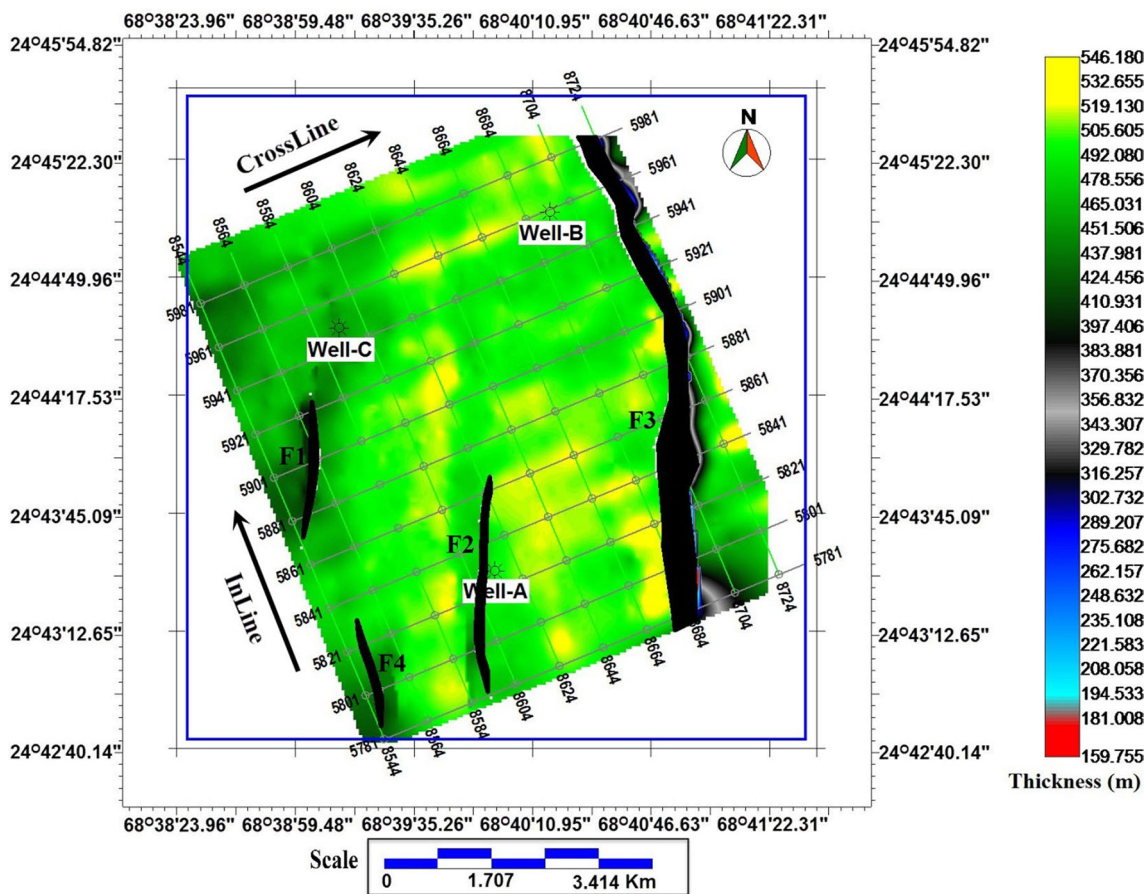


**Fig. 9** Isopach map of the Sembar Formation showing its thickness variation. *F1, F2, F3* and *F4* represent the faults traced over the base map. The color legend provides the information about lateral variation in thickness of the Sembar Formation

**Table 2** Estimated values of TOC from Passey's and Schwarzkopf's methods for all the three wells

Wells	Depth (m)	LOM	Baseline values		Average TOC (wt%) by Passey's method	Average TOC (wt%) Schwarzkopf's method
			Resistivity ( $\Omega m$ )	Sonic ( $\mu s/ft$ )		
A	2400–2840	10.5	2	85	2.5	3.7
B	2400–2840	9.5	7	70	2.2	2.2
C	2510–2800	8.5	8	70	4	2.3

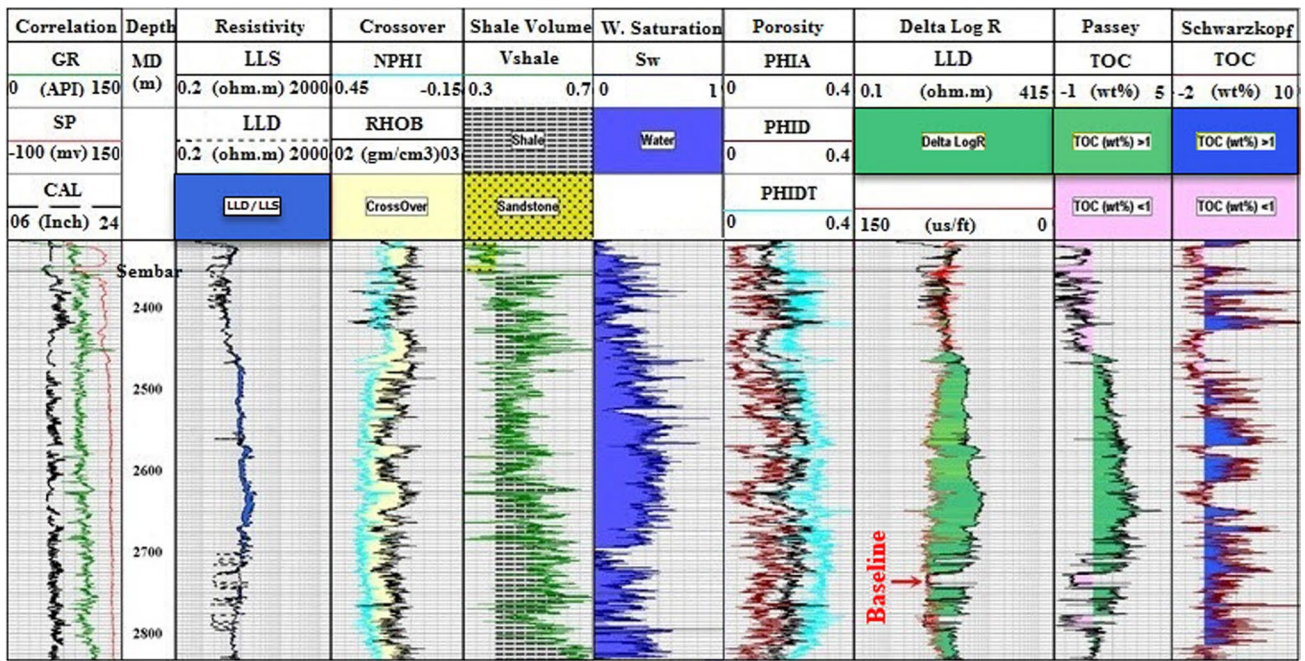


**Fig. 10** TOC values (wt%) estimated from Passey’s  $\Delta\log R$  and Schwarzkopf’s methods in Well A (track 8 and 9). Track 1 is a lithological track, track 2 is a resistivity track and track 3 is a porosity track. The rest of the tracks represent the derived reservoir properties

(shale volume, water saturation, porosities, and Delta LogR) that are used to calculate TOC (wt%) curves from both methods (tracks 8 and 9)

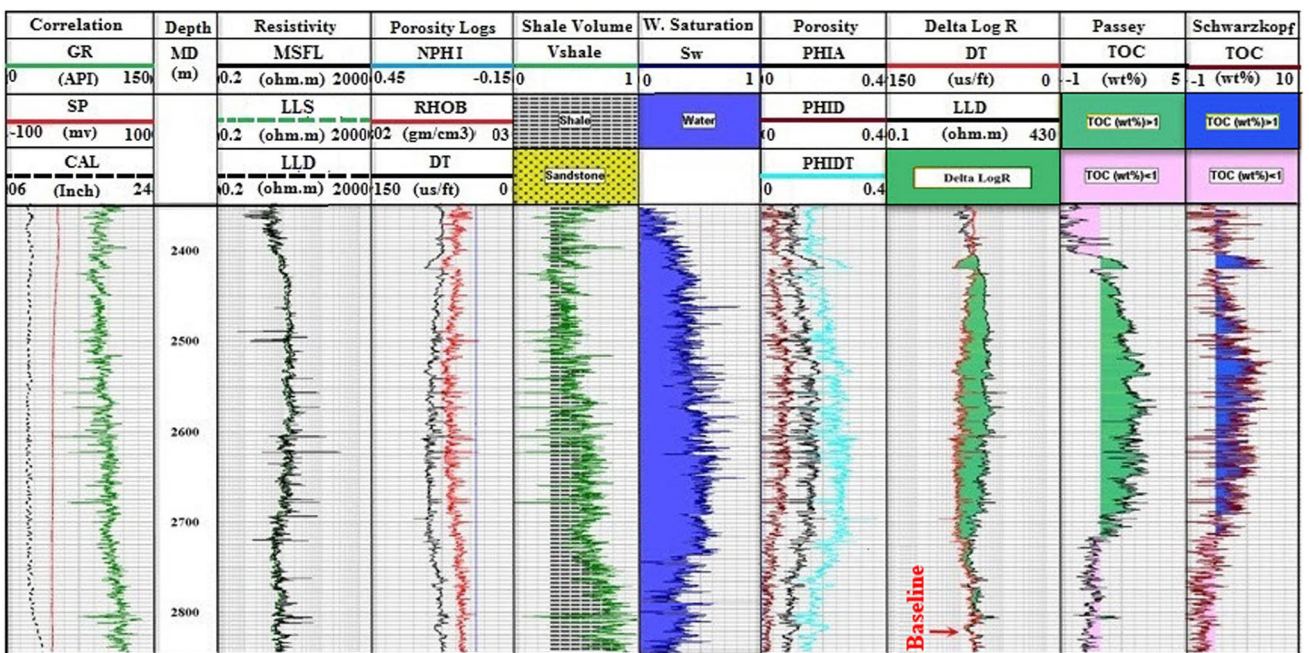


**Fig. 11** TOC values (wt%) estimated from Passey’s  $\Delta\log R$  and Schwarzkopf’s methods in Well B (track 8 and 9). Track 1 is a lithological track, track 2 is a resistivity track and track 3 is a porosity track. The rest of the tracks represent the derived reservoir properties

(shale volume, water saturation, porosities, and Delta LogR) that are used to calculate TOC (wt%) curves from both methods (tracks 8 and 9)

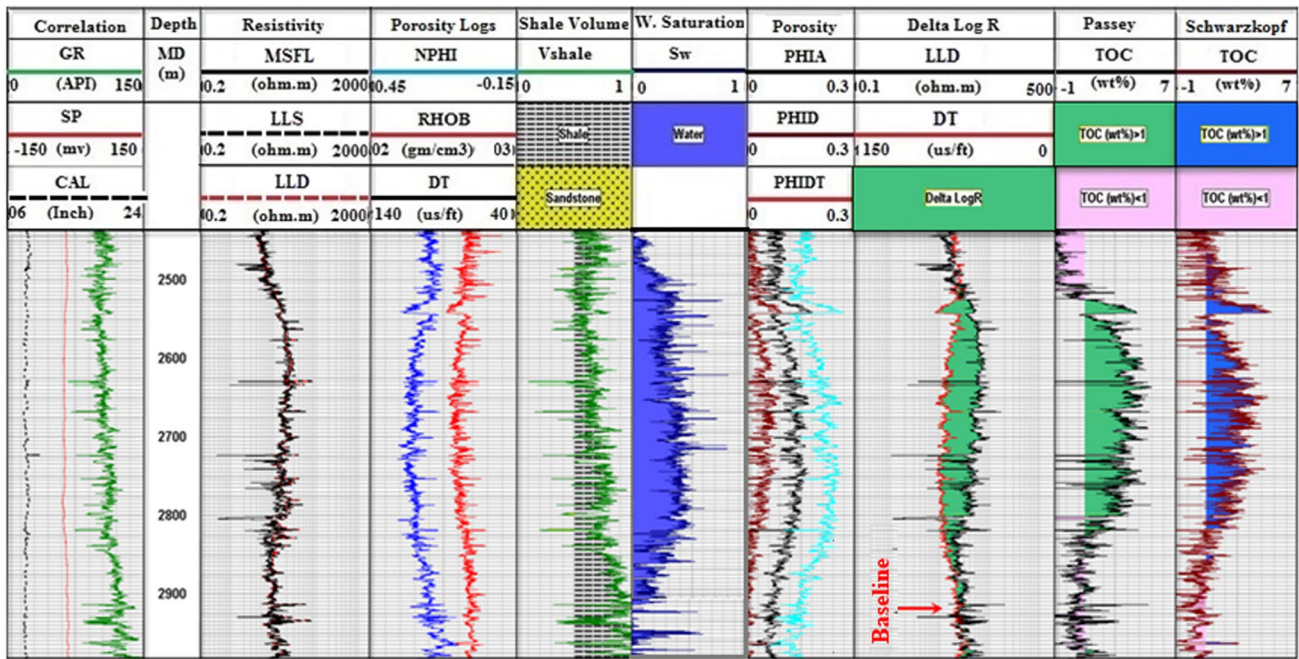


Fig. 12 TOC values (wt%) estimated from Passey’s  $\Delta\log R$  and Schwarzkopf’s methods in Well C (track 8 and 9). Track 1 is a lithological track, track 2 is a resistivity track and track 3 is a porosity track. The rest of the tracks represent the derived reservoir properties

(shale volume, water saturation, porosities, and Delta LogR) that are used to calculate TOC (wt%) curves from both methods (tracks 8 and 9)

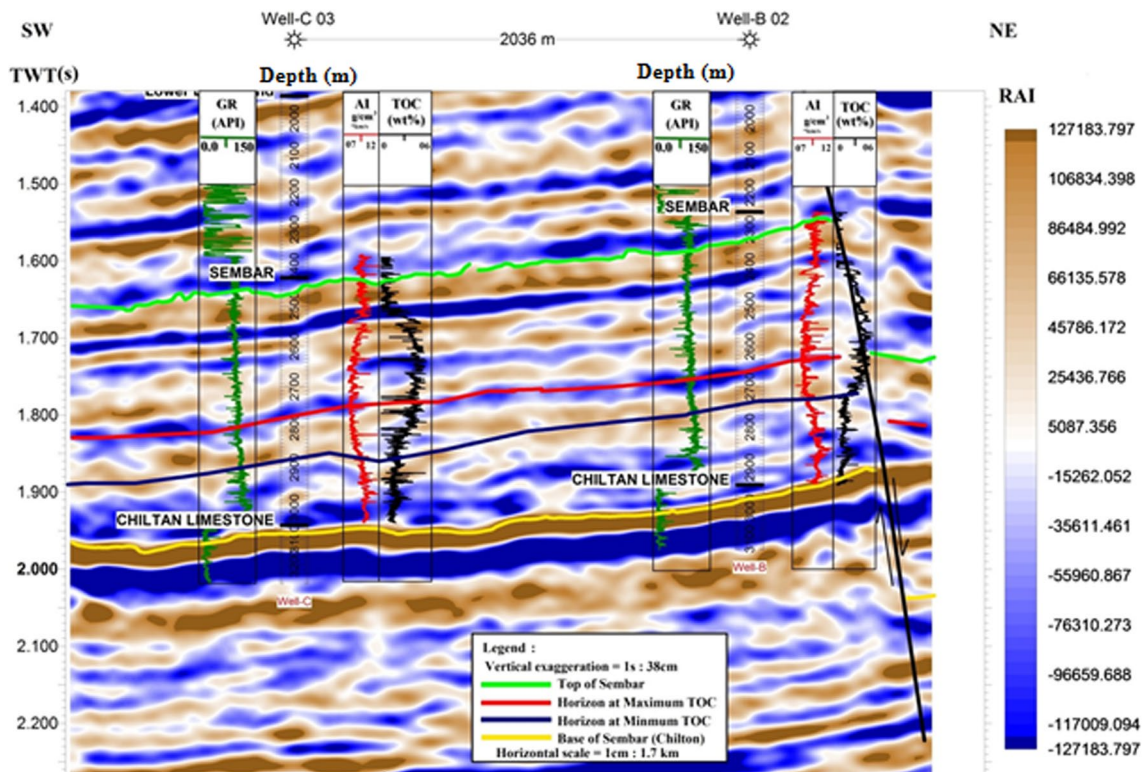


Fig. 13 Interpreted seismic section of in-line 5941 with a display of GR (green), AI (red) and TOC (black) curves at the location of well B and C for calibration purpose. The red horizon is picked at maximum

TOC (low RAI) interval, while the blue horizon is picked minimum TOC (high RAI) interval within the Sembar Formation

### Analysis of TOC from seismic data

To analyze TOC from seismic data, the amplitude information in the seismic cube is converted into RAI values using Eq. (6) and calibrated with the AI and TOC curves calculated from well log data (Fig. 13). The identified low and high TOC zones with the Sembar Formation are gridded in terms of RAI as discussed in Section "Seismic based TOC estimation". From the RAI maps, one can clearly see the distribution of low and high acoustic impedances at well locations in Figs. 14, 15, which can be related to high and low TOC. The estimation of TOC from the RAI converted maps needs a relationship in the form of cross-plot between logs derived TOC and seismic derived RAI. The cross-plot of TOC and RAI gives inverse relation with a correlation coefficient  $R^2 = 0.72$  (Fig. 16). In particular, the data in this cross-plot comes from both high/low TOC and RAI zones and the resulting linear relationship is used for the estimation of both high and low TOC zones within the Sembar Formation. In addition to that, we have used the estimated values of TOC from the Passey’s method in cross-plot analysis.

The Passey’s method is used, as the estimated TOC values involve the incorporation of laboratory/core data along with well log data making it more reliable than Schwarzkopf’s method, which depends only on the well log data i.e. RHOB log. The Equation of the best fit line representing the general trend between TOC and RAI is given as

$$TOC = -10^{-5} RAI + 1.7356. \tag{7}$$

Finally, TOC maps are generated from RAI maps using Eq. (7) (Fig. 17). The estimated TOC values from seismic data show good calibration with well log data and suggest that Sembar Formation has suitable potential within the shale gas perspective (Table 2; Fig. 17). Moreover, we have also shown an estimation of TOC using RAI extracted at a low TOC and high acoustic impedance zone (Fig. 18). By examining the behavior of RAI and TOC at well locations in Figs. 14, 15, 17 and 18, it can be observed that high and low TOC indeed manifests itself in terms of RAI anomalies. In particular, high TOC at well locations in Fig. 17 show low RAI in Fig. 14 and low TOC at well locations in Fig. 18 show high RAI in Fig. 15.

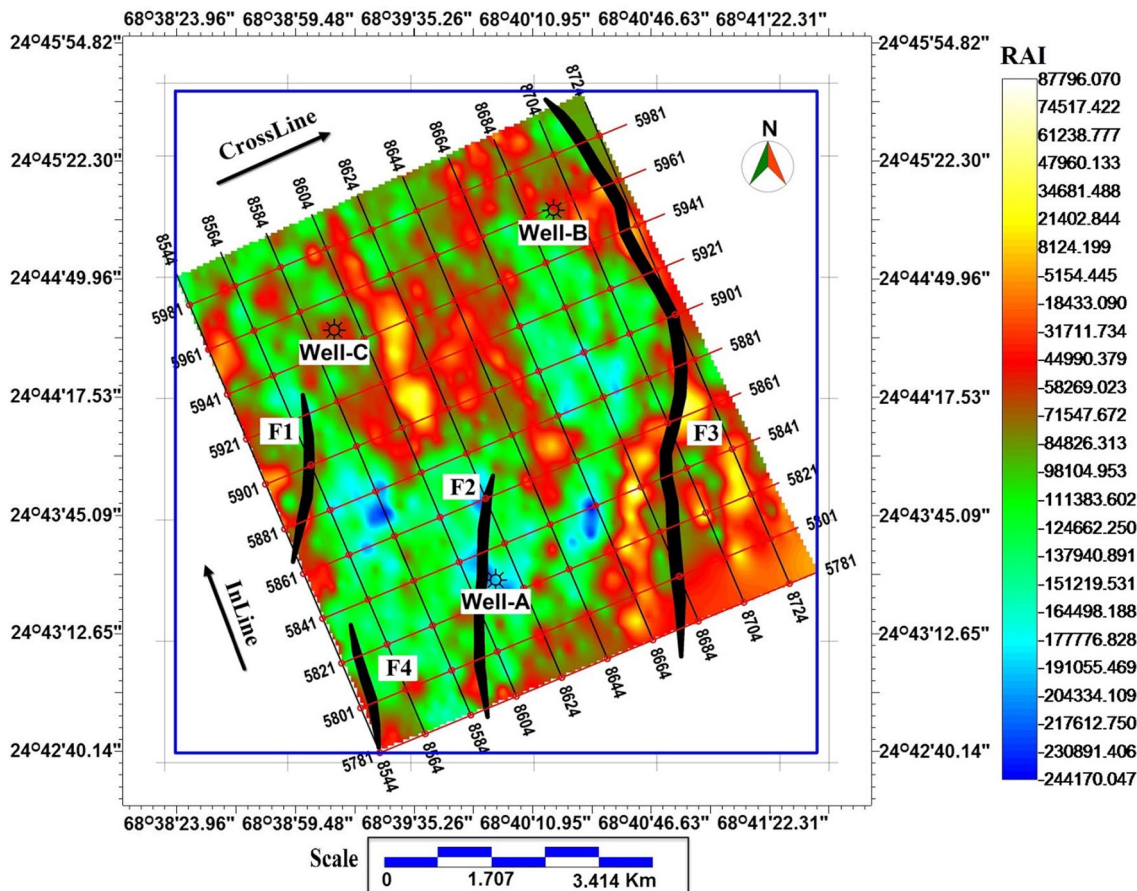


**Fig. 14** RAI extracted at a 25×25 m grid along the maximum TOC zone of Sembar Formation. The map shows low RAI values at the location of wells A, B and C

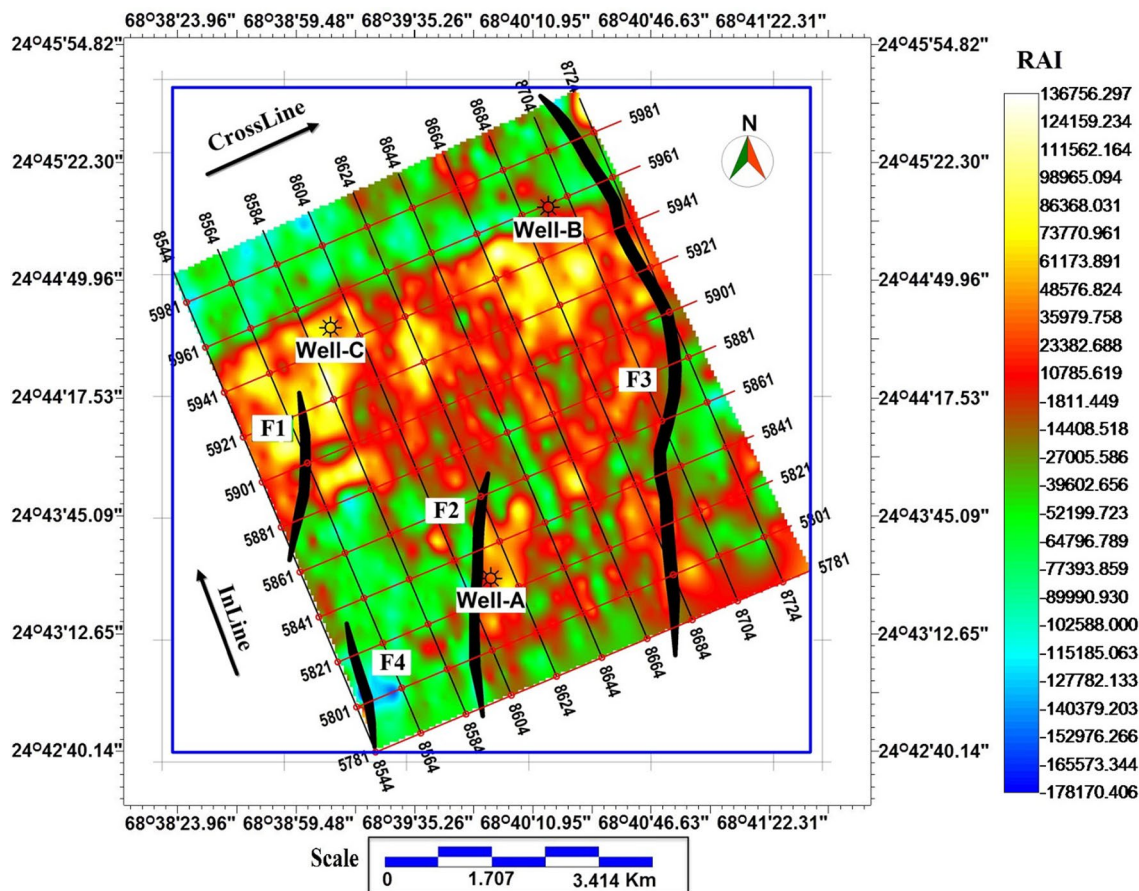


**Fig. 15** RAI extracted at a  $25 \times 25$  m grid along the minimum TOC zone of Sembar Formation. The map shows high RAI values at the location of wells A, B and C

## Discussions

Overall, the estimated TOC values for the Sembar Formation in this study ranges from 1 to 4 wt% showing that it lies in the range of good to excellent source rock (Peters et al. 1986). The values of TOC of the Sembar Formation analyzed by Wandrey et al. (2004) from laboratory samples range from 0.5 to 3.5 wt%. So the result of the TOC obtained in this work shows a good agreement with study conducted by Wandrey et al. (2004). It is further inferred that Kerogen of the Sembar Formation is mostly of Type-II and III in the Lower and Middle Indus Basin (Wandrey et al. 2004; Ahmad et al. 2011). The TOC values calculated from seismic data for the Sembar Formation increases from eastern to western side (Fig. 17). Thermally, the rock is much more mature to the western part of the shelf due to deep burial depth and less mature to the eastern part due to shallow burial depth (Fig. 8; Wandrey et al. 2004).

Our analysis shows that the Sembar Formation can act as a good potential unconventional resource because it is much mature towards higher concentration of TOC

(Fig. 17). The reason for the high concentration of TOC is the paleo-geographic location of the Sembar Formation during its depositional time. The age and depositional environment as discussed in Geologic settings suggest that during the late Jurassic and Lower Cretaceous, the Indian plate drifted northward, entering to warmer latitude (Scotese et al. 1988). On its lower shelf, marine shales of the Lower Cretaceous Sembar Formation were deposited over Jurassic age Chiltan Limestone. During this age, the paleo-geographic latitude of the Indian plate was at location of nearly Latitude  $20^{\circ}\text{S}$  and Longitude  $68^{\circ}\text{E}$  (Scotese et al. 1988). The higher concentration of TOC suggests that the existed paleo-environment at that time was suitable for high productivity rate of organic matter. Furthermore, it can also be further inferred that, it was the time when the decomposition rate was slow (means an anoxic environment suitable for preservation of the organic matter existed) as compared to the productivity rate of the organic matter resulting in such high concentration of TOC. The rich TOC potential of the Sembar Formation makes it a

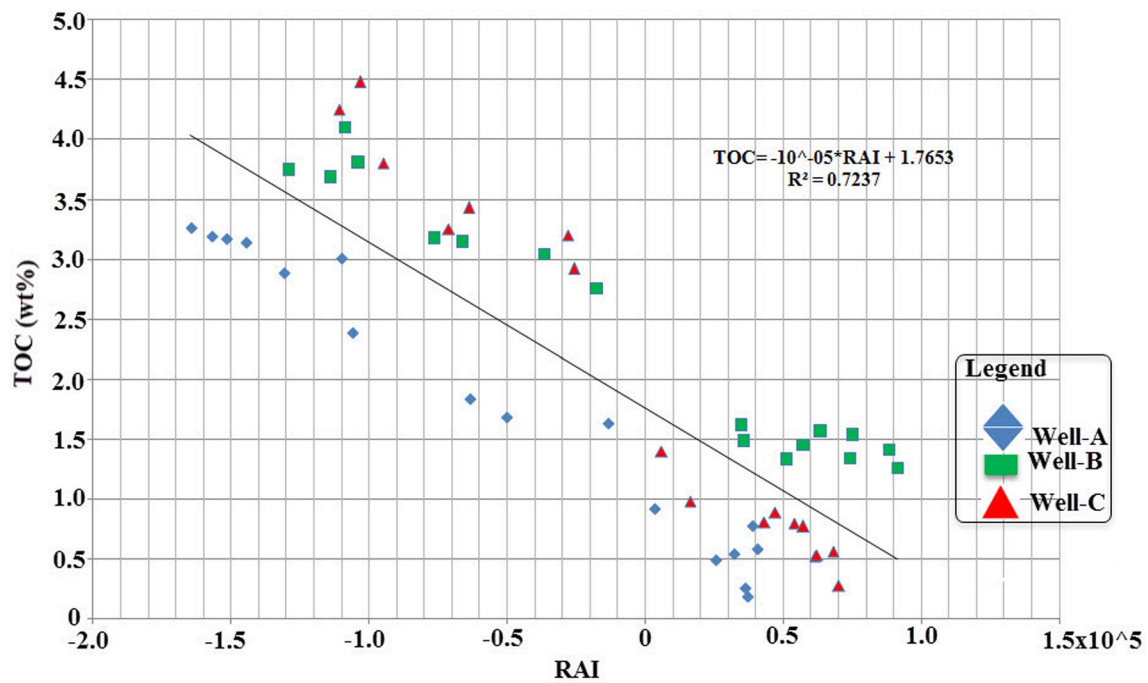


**Fig. 16** A linear relationship established via a cross-plot between TOC (estimated from well data) and extracted RAI (from seismic) at the location of all the three wells. In particular, both high/low TOC

and RAI zones within the Sembar Formation are used. The linear relationship established in the cross-plot is then used for the estimation of TOC from seismic based extracted RAI values

potential source rock and as well as a potential unconventional play.

For further evaluation of the unconventional potential of a particular unit, the depth of exploitation and its thickness is an essential target. In platform areas, such as the Lower and Middle Indus Basins, the general economic exploitation depths for shale gas are about 3500 m, while that in tectonically unstable fold-belts, it ranges from 1000 to 3000 m (Ahmad et al. 2011). The exploitation depth of Sembar Formation obtained for our study starts from around 2200 m (Fig. 8) having considerable thickness (Fig. 9), making it a feasible and suitable candidate for unconventional resource exploitation with higher concentration of TOC (Fig. 17).

The analogues of Sembar Formation are present in the Rajasthan Basin (eastern side of the study area) of the Indian subcontinent and in the Zagros fold-belt of Iran (western side of the study area) (Klett et al. 2011; Opera et al. 2013). These analogues units are the most productive source rocks of their respective basins within the context of shale gas exploitation (Klett et al. 2011; Opera et al. 2013). The values of the TOC in the Gurpi and Kazdumi Formation of Zagros fold-belt of Iran ranges from 1.7 to 2.4 wt% and 1.5 to 3.92 wt% respectively (Opera et al. 2013). The source potential of the Ghaggar–Hakra Formation of Rajasthan Basin is poorly known due to limited number of well penetrations (Farrimond et al. 2015). We expect that this methodology

may be helpful in exploration of unconventional resources for such basins worldwide.

## Conclusions

The Sembar Formation is an ideal shale gas prospect of the Lower Indus Basin in terms of depositional environment, thickness, organic geochemistry, thermal maturity, mineralogy and porosity. One of the key features for successful shale gas plays requires high TOC. In this study, we have devised a methodology for estimation of TOC from seismic and well log data for the Sembar Formation in Badin area, Lower Indus Basin, Pakistan. The extracted maps of RAI and estimated TOC (1–4%) within the Sembar Formation are evaluated on the reservoir scale with a good correlation coefficient. The estimated TOC values for Sembar Formation show that it lies in the range of good to excellent potential shale oil/gas reservoir. Our results suggest that high and low TOC values indeed manifest themselves in terms of RAI anomalies. Moreover, the results also suggest an excellent calibration of TOC values from seismic at well locations. We anticipate that this methodology can be helpful in the initial assessment and identification of optimum sweet spots (high TOC) for shale gas plays worldwide.

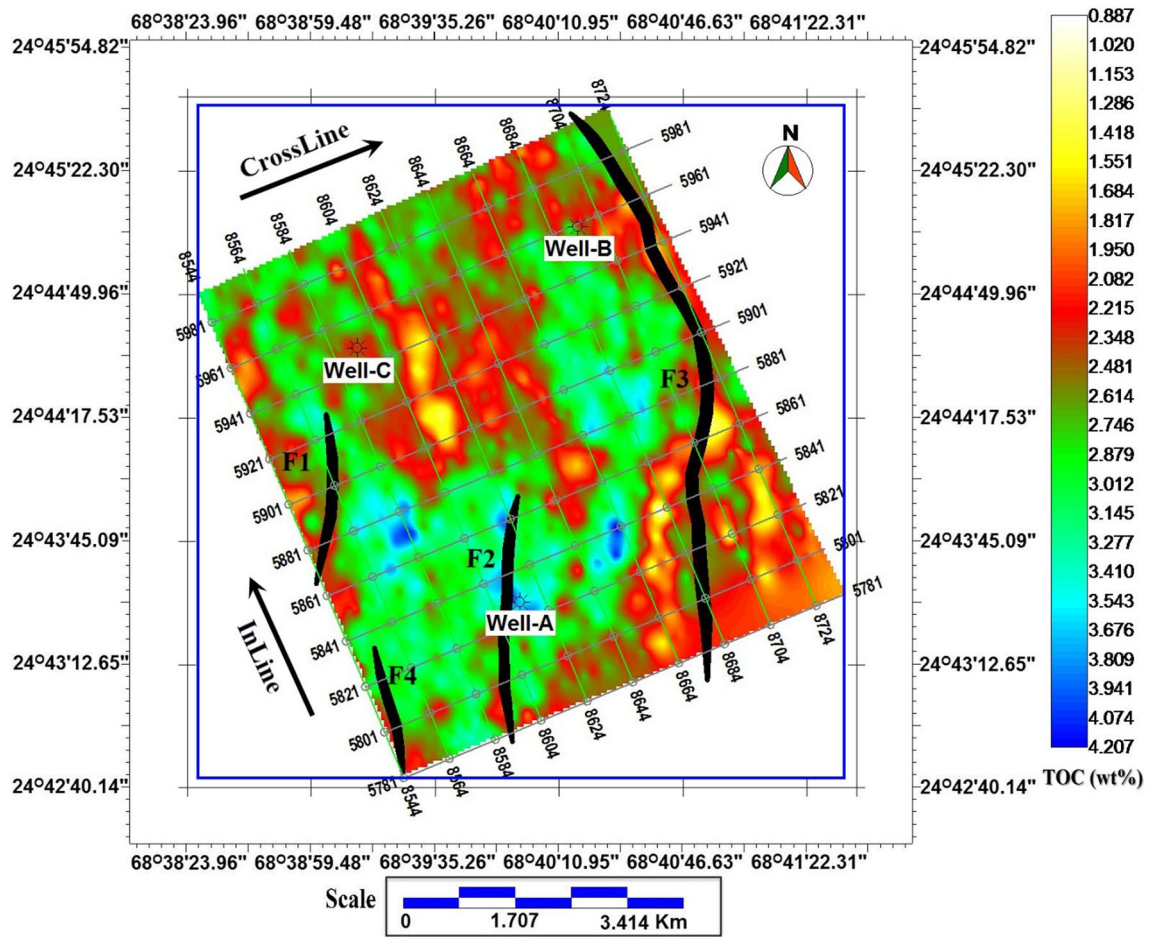


**Fig. 17** Seismic based TOC using Passey’s method for RAI extracted along high TOC and low acoustic impedance zone within the Sembar Formation. The map shows high TOC values at the locations of wells A, B and C



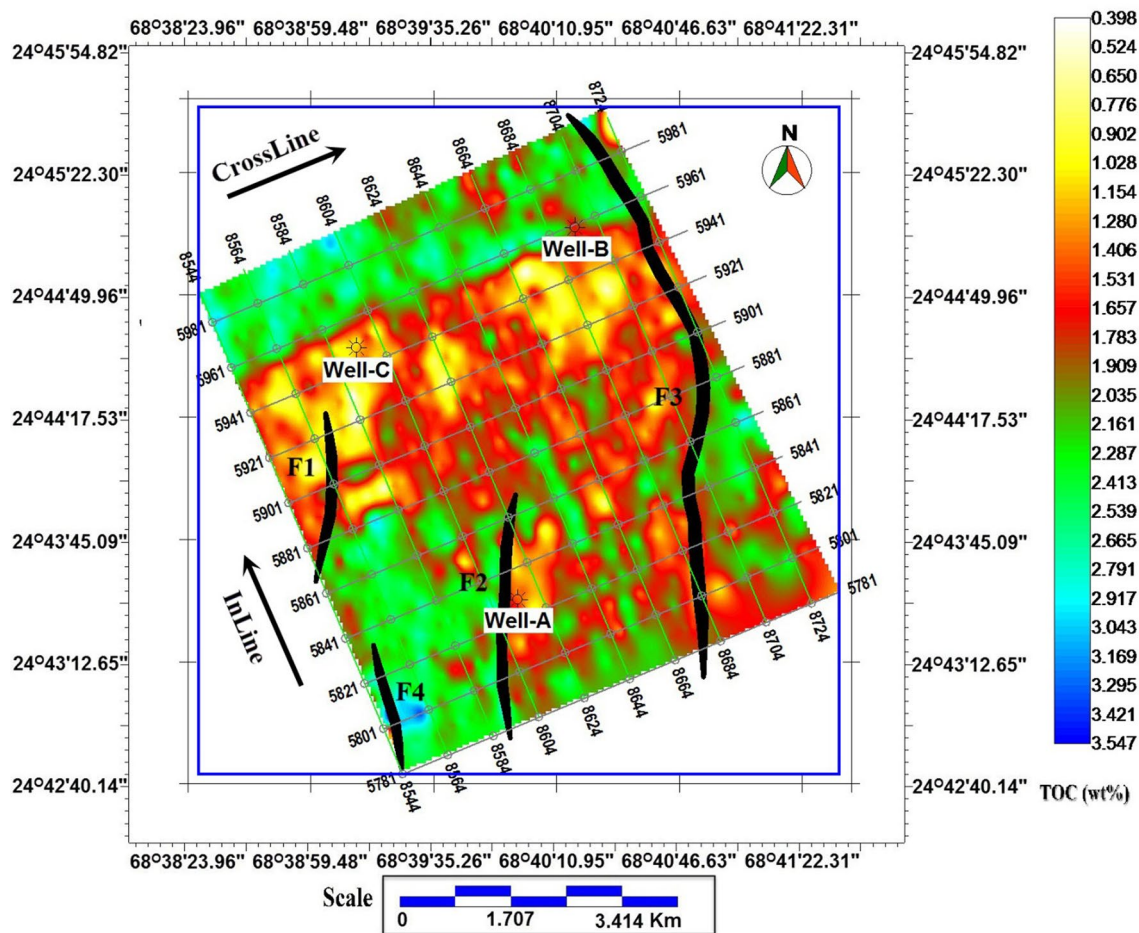


**Fig. 18** Seismic based TOC using Passey's method for RAI extracted along low TOC and high acoustic impedance zone within the Sembar Formation. The map shows low TOC values at the locations of wells A, B and C

**Acknowledgements** Dr. Aamir Ali would like to thank Higher Education Commission (HEC), Pakistan for providing basic funding via its NRP program (Grant No. 4115) required to complete this work. Mr. Omer Aziz would like to thank Directorate General of Petroleum Concessions (DGPC), Pakistan, for allowing the use of seismic and well log data for research and publication purposes and Department of Earth Sciences, Quaid-i-Azam University, Islamabad, Pakistan for providing the basic requirements to complete this work. The authors would also like to thank reviewers for their insightful comments on the paper, as these comments led us to an improvement of the work.

## References

- Abbasi AH, Mehmood F, Kamal M (2014) Shale oil and gas: lifeline for Pakistan. Sustainable Development Policy Institute, Islamabad, pp 85–87
- Abbasi SA, Kalwar Z, Solangi SH (2016) Study of structural styles and hydrocarbon potential of RajanPur Area, Middle Indus Basin, Pakistan. *Bu J ES* 1(1):36–41
- Ahmad N, Mateen J, Shehzad K, Mehmood N, Arif F (2011) Shale gas potential of Lower Cretaceous Sembar Formation in Middle and Lower Indus Basin, Pakistan. In: *Assoc Pet Geol/Soc Pet Explor-Ann Tech Confer*, pp 235–252
- Alam MSM, Wasimuddin M, Ahmad SSM (2002) Zaur structure, a complex trap in poor seismic data area, BP Pakistan Exploration and Production Inc. PAPG/SPE ATC conference. Islamabad, Pakistan, pp 1–3
- Bacon M, Simm R, Redshaw T (2007) 3-D seismic interpretation. Cambridge University, Cambridge
- Biswas SK (1987) Regional tectonic framework, structure and evolution of the western marginal basins of India. *Tectonophysics* 135(4):307–327
- Bocora J (2012) Global prospects for the development of unconventional gas. *Proced-Soc Behav Sci* 65:436–442
- Bowman T (2010) Direct method for determining organic shale potential from porosity and resistivity logs and identify possible resource play. In: *AAPG annual convention*, New Orleans, pp 11–14
- Eickhoff G, Alam S (1991) On the petroleum geology and prospectivity of Kirther Range and Sibi Trough, Southern Indus Basin, Pakistan. BGR/HDIP, Hannover
- Farah AG, Lawrence RD, De J (1984) An overview of the tectonics of Pakistan. In: Haq BU, Mil Liman JD (eds), *Marine geology and oceanography of the Arabian Sea and coastal Pakistan*. Van No Strand and Reinhold Co., New York, pp 161–176
- Farrimond P, Naidoo SB, Burley SD, Dolson J, Whiteley N, Kothari V (2015) Geochemical characterization of oils and their source

- rocks in the Barmer Basin, Rajasthan, India. *Pet GeoSoc* 21:301–321
- Fertl WH, Chilingar GV (1988) Total organic content determined from well logs. *SPE/ATC Exhib* 3:407–419
- Fertl WH, Rieke HH (1980) Gamma ray spectral evaluation techniques identify fractured shale reservoir and source-rock characteristic. *J Pet Technol* 31:2053–2062
- Gluyas J, Swarbrick R (2009) *Petroleum geoscience*. Blackwell, Malden
- Guidry FK, Walsh JW (1993) Well log interpretation of a Devonian gas shale: an example analysis. In: *SPE Eastern Regional Meeting, Society of Petroleum Engineers*
- Hood A, Gutjahr CCM, Heacock RL (1975) Organic metamorphism and generation of petroleum. *AAPG Bull* 59:986–996
- Iqbal MWA, Shah SMI (1980) A guide to stratigraphy of Pakistan, vol 53. *GSP, Quetta*
- Jianliang J, Zhaojun L, Qingtao M, Rong L, Pingchang S, Yongcheng C (2012) Quantitative evaluation of oil shale based on well log and 3-D seismic technique in the Songliao Basin, Northeast China. *Oil Shale* 29(2):128–150
- Kadri IB (1995) *Petroleum geology of Pakistan*. Pakistan Petroleum Limited, Karachi, pp 35–37
- Kazmi AH, Snee LW (1989) *Geology of world emerald deposits: a brief review*. Van Nostrand Reinhold, The Netherlands, pp 165–228
- Kefferpütz R (2010) Shale fever: replicating the US gas revolution in the EU? *CEPS Policy Brief* No. 210, 17 June
- Klett TR, Schenk CJ, Wandrey CJ, Brownfield M, Charpentier RR, Cook T, Gautier DL, Pollastro RM (2011) Assessment of potential shale gas resources of the Bombay, Cauvery, and Krishna–Godavari Provinces, India. *USGS Fact Sheet*, pp 3131–3132
- Liu L, Shang X, Wang P, Guo Y, Wang W, Wu L (2012) Estimation on organic carbon content of source rocks by logging evaluation method as exemplified by those of the 4th and 3rd members of the Shahejie Formation in Western Sag of Liaohe Oilfield. *Chin J Geochem* 31(4):398–407
- Løseth H, Wensaas L, Gading M, Duffaut K, Springer M (2011) Can hydrocarbon source rocks be identified on seismic data? *Geology* 39(12):1167–1170
- Meissner FF (1978) *Petroleum geology of the Bakken Formation, Williston Basin, North Dakota and Montana*. In: *Geological Society. The economic geology of the Williston basin; Montana, North Dakota, South Dakota*, pp 207–227
- Meyer BL, Nederlof MH (1984) Identification of source on wire-line logs by density/resistivity and sonic transit time/resistivity crossplot. *AAPG Bull* 68:121–129
- Miller RG, Sorrell SR (2014) The future of oil supply. *Philos Trans R Soc* 372 (2006):1–27
- Munir A, Asim S, Bablani S, Asif A (2014) Seismic data interpretation and fault mapping in Badin Area, Sindh, Pakistan. *SURJ* 46(2):133–142
- Myers KJ, Jenkyns KF (1992) Determining total organic carbon content from well logs: an inter comparison of GST data and a new density log method. *Geol Soc London Spec Publ*, 65:369–376
- Nissen SE, Carr TR, Marfurt KJ, Sullivan EC (2009) Using 3-D seismic volumetric curvature attributes to identify fracture trends in a depleted Mississippian carbonate reservoir: implications for assessing candidates for CO<sub>2</sub> sequestration. *AAPG Special Volumes*, pp 297–319
- Nixon RP (1973) Oil source beds in Cretaceous Mowry Shale of Northwestern Interior United States. *AAPG* 57(1):136–157
- Opera A, Alizadeh B, Sarafdokht H, Janbaz M, Fouladvand R, Heidarifard MH (2013) Burial history reconstruction and thermal maturity modeling for the middle cretaceous–early miocene petroleum System, southern Dezful Embayment, SW Iran. *Int J Coal Geol* 120:1–14
- Passey QR, Creaney S, Kulla JB, Moretti FJ, Stroud JD (1990) A practical model for organic richness from porosity and resistivity logs. *AAPG Bull* 74:1777–1794
- Passey QR, Bohacs KM, Esch WL, Klimentidis R, Sinha S (2010) From oil-prone source rock to gas-producing shale reservoir—geologic and petrophysical characterization of unconventional shale-gas reservoirs conference, Beijing, 8 June.
- Peters KE (1986) Guidelines for evaluating petroleum source rock using programmed pyrolysis. *AAPG Bull* 70(3):318–329
- Philippi GT (1968) Essentials of the petroleum formation process are organic source material and a subsurface temperature controlled chemical reaction mechanism, in *advances in organic geochemistry*. Pergamon, Oxford, pp 25–46
- Raza HA, Ali SM, Ahmed R, Ahmed J (1990) *Petroleum geology of Kirther Sub-Basin and part of Kutch Basin*. *Pak J Hydrocarbon Res* 2(1):29–73
- Rezaee R (2015) *Fundamentals of gas shale reservoirs*. Wiley, Hoboken, pp 191–245
- Rider MH (2002) *The geological interpretation of well logs*, 2nd edn. Rider-French Consulting Limited, Rogart, pp 42–147
- Rybach L (1986) Amount and significance of radioactive heat sources in sediments. *Collect Colloq Semin* 44:311–322
- Schmoker JW (1981) Organic-matter content of Appalachian Devonian shales determined by use of wire-line logs: summary of work done 1976–1980. *Geological Survey, Reston*, pp 81–181
- Schwarzkopf TA (1992) Source rock potential (TOC + hydrogen index) evaluation by integrating well log and geochemical data. *Org Geochem* 19(4):545–555
- Scotese CR, Gahagan LM, Larson RL (1988) Plate tectonic reconstructions of the Cretaceous and Cenozoic ocean basins. *Tectonophysics* 155:27–48
- Shahzad K, Betzler C, Ahmed N, Qayyum F, Spezzaferri S, Qadir A (2017) Growth and demise of a Paleogene isolated carbonate platform of the Offshore Indus Basin, Pakistan: effects of regional and local controlling factors. *Int J Earth Sci* 2017:1–24
- Sunjay (2011) *Shale gas: an unconventional reservoir. Recovery—2011 CSPG CSEG CWLS Convention*, pp 1–4
- Wandrey CJ, Law BE, Shah AH (2004) Sembar Goru/Ghazij composite total petroleum system, Indus and Sulaiman-kirther Geological Province, Pakistan and India. *USGS Bulletin*, pp 1–23
- Wood DA (1988) Relationship between thermal maturity indices calculated using Arrhenius equation and Lopatin method: implications for petroleum exploration. *AAPG Bull* 72:115–134
- Zou C, Zhao Q, Zhang G, Xiong B (2016) Energy revolution: From a fossil energy era to a new energy era. *Nat Gas Ind Bull* 3(1):1–11